Chapter 2
Images for X-ray Testing

Abstract In this chapter, we present the dataset that is used in this book to illustrate and test several methods. The database consists of 19,407 X-ray images. The images are organized in a public database called GDXray that can be used free of charge, but for research and educational purposes only. The database includes five groups of X-ray images: castings, welds, baggage, natural objects, and settings. Each group has several series, and each series several X-ray images. Most of the series are annotated or labeled. In such cases, the coordinates of the bounding boxes of the objects of interest or the labels of the images are available in standard text files. The size of GDXray is 3.5 GB and it can be downloaded from our website.

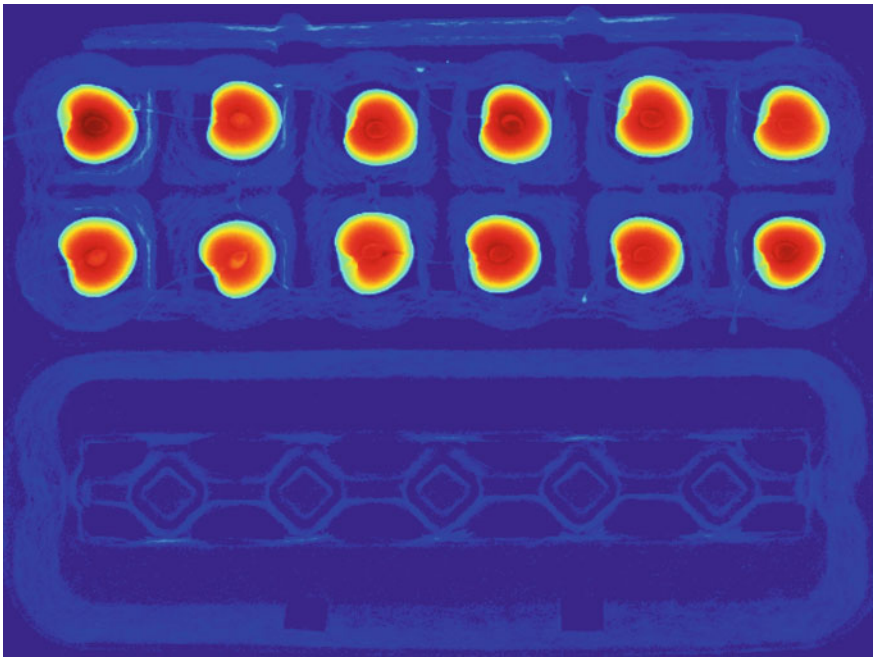

Cover image: *X-ray image of cherries in an egg crate (X-ray image* `N0006_0027` *colored with 'jet' colormap).*

D. Mery, *Computer Vision for X-Ray Testing*, DOI 10.1007/978-3-319-20747-6_2

2.1 Introduction

Public databases of X-ray images can be found for medical imaging,[1] however, to the best knowledge of the author, up until now there have not been any public databases of digital X-ray images for X-ray testing.[2]

As a service to the X-ray testing community, we collected more than 19,400 X-ray images for the development, testing and evaluation of image analysis and computer vision algorithms. The images are organized in a public database called 𝔾𝔻𝕏ray.[3] In order to illustrate our database, a random selection of 120 X-ray images is shown in Fig. 2.1. The database includes five groups of X-ray images: castings, welds, baggage, natural objects, and settings. Each group has several series, and each series several X-ray images. Some samples of each series are illustrated in Fig. 2.2. Most of the series are annotated or labeled. In those cases, the coordinates of the bounding boxes of the objects of interest or the labels of the images are available. In Table 2.1, we can see some statistics. The size of 𝔾𝔻𝕏ray is 3.49 GB and it can be downloaded from our website (see Fig. 2.2).

In this chapter, we will view the structure of 𝔾𝔻𝕏ray database, a description for each group (with some series examples), some examples of applications that have been published using images of 𝔾𝔻𝕏ray and some examples in Matlab that can be used to manipulate the database. More details about 𝔾𝔻𝕏ray are given in Appendix A.

2.2 Structure of the Database

𝔾𝔻𝕏ray is available in a public repository. The repository contains five group folders one for each group: `Castings`, `Welds`, `Baggage`, `Nature`, and `Settings`. For each group we define an initial: `C`, `W`, `B`, `N`, and `S`, respectively. As shown in Table 2.1, each group has several series. Each series is stored in an individual subfolder of the corresponding group folder. The subfolder name is `Xssss`, where `X` is the initial of the group and `ssss` is the number of the series. For example, the third series of group Castings is stored in subfolder `C0003` of folder `Castings` (see more examples in Fig. 2.2). The X-ray images of a series are stored in file `Xssss_nnnn.png`. Again

[1] See for example a good collection in http://www.via.cornell.edu/databases/.

[2] There are some galleries of X-ray images available on the web with a few samples, see for instance http://www.vidisco.com/ndt_solutions/ndt_info_center/ndt_x_ray_gallery with approximately 50 X-ray images.

[3] Available on http://dmery.ing.puc.cl/index.php/material/gdxray. The name comes originally from 'The Grima X-ray database' (Grima is the name of our Machine Intelligence Group at the Department of Computer Science of the Pontificia Universidad Católica de Chile http://grima.ing.puc.cl). The X-ray images included in 𝔾𝔻𝕏ray can be used free of charge, but for research and educational purposes only. Redistribution and commercial use is prohibited. Any researcher reporting results which use this database should acknowledge the 𝔾𝔻𝕏ray database by citing [1].

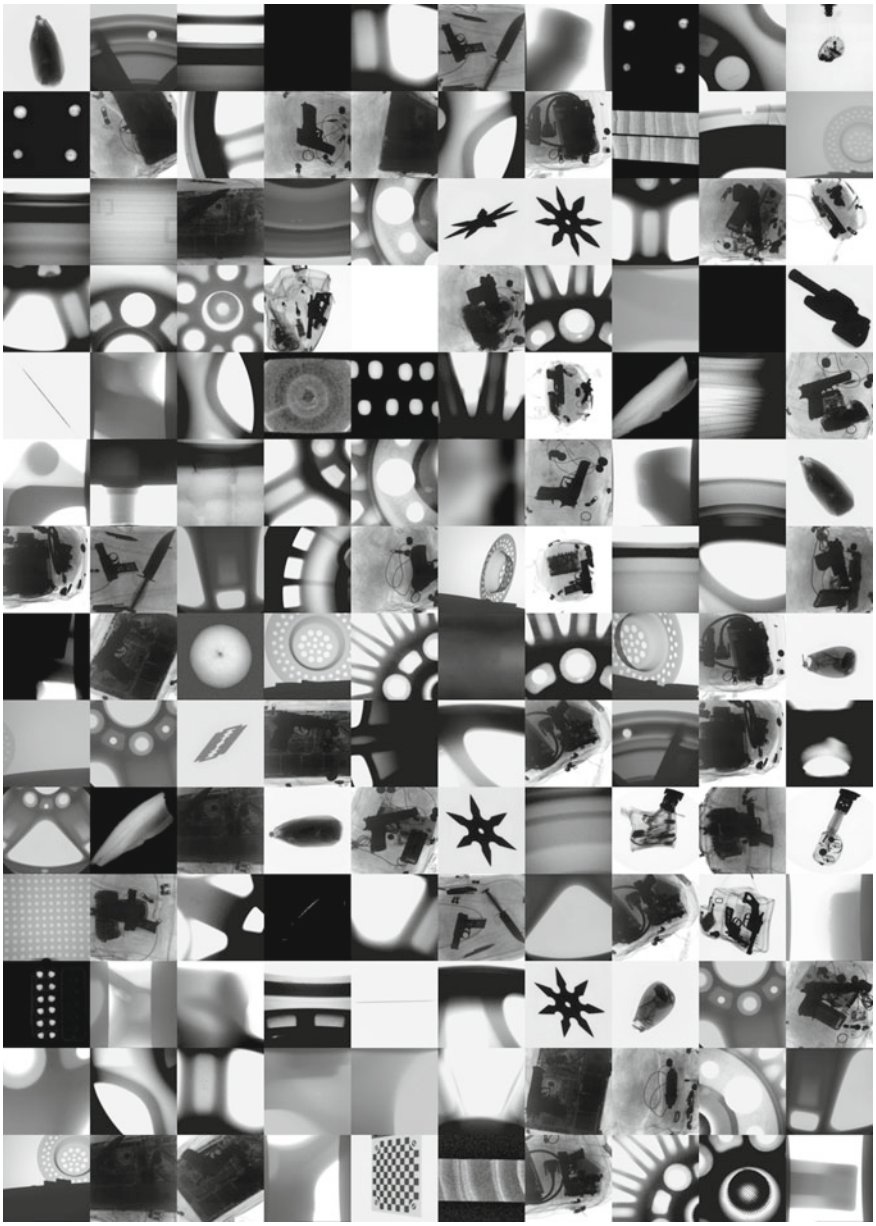

Fig. 2.1 Random X-ray images of GDXray database

`Xssss` is the name of the series. The number `nnnn` corresponds to the number of the X-ray image of this series. For example, the fifth X-ray image of series `C0003` is `C0003_0005.png` and is stored in folder `Castings/C0003`. The whole

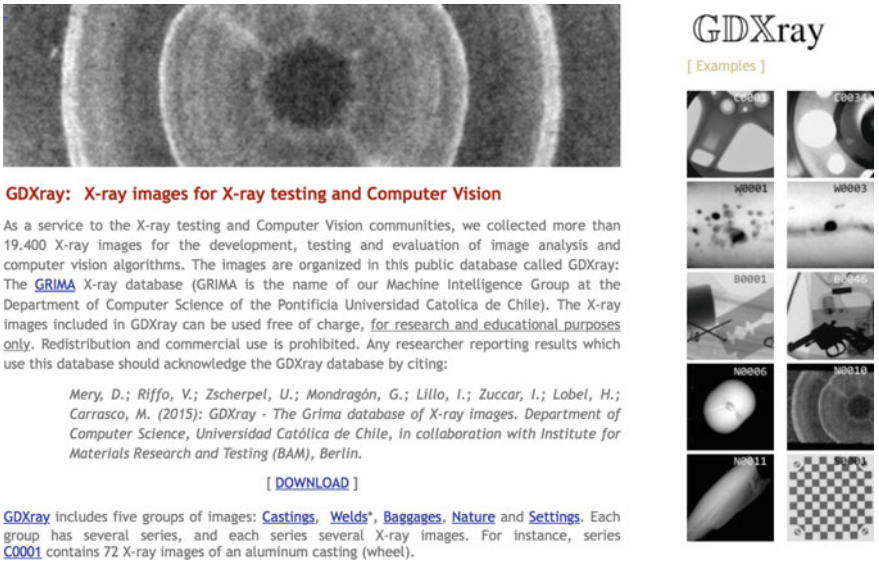

Fig. 2.2 Screenshot of GDXray website. Some X-ray images of ten series are shown at the *right-hand side*: `C0001` and `C0034` for castings, `W0001` and `W0003` for welds, `B0001` and `B0046` for baggage, `N0006` (cherry), `N0010` (wood), and `N0011` (salmon) for natural objects and `S0001` for settings (a calibration pattern)

Table 2.1 Statistics of GDXray database

Groups	Series	Images	Size (MB)
Castings	67	2,727	307.5
Welds	3	88	209.4
Baggage	77	8,150	2,734.8
Nature	13	8,290	191.9
Settings	7	152	45.5
Total	167	19,407	3,489.0

structure is summarized in Table 2.2. All X-ray images of GDXray are stored in 'png' (Portable Network Graphics)[4] format.

2.3 Castings

The group Castings contains 2,727 X-ray images arranged in 67 series. The X-ray images were taken mainly from automotive parts (aluminum wheels and knuckles). Some examples are illustrated in Figs. 2.3, 2.4 and 2.5. The details of each series are

[4] See http://www.libpng.org/pub/png/.

Table 2.2 Structure of GDXray

Database	Groups	Series	X-ray images
GDXray →	Castings →	C0001 →	C0001_0001.png ... C0001_0072.png
		:	
		C0067 →	C0067_0001.png ... C0067_0083.png
	Welds →	W0001 →	W0001_0001.png ... W0001_0010.png
		:	
		W0003 →	W0003_0001.png ... W0003_0068.png
	Baggage →	B0001 →	B0001_0001.png ... B0001_0014.png
		:	
		B0077 →	B0077_0001.png ... B0077_00576.png
	Nature →	N0001 →	N0001_0001.png ... N0001_0013.png
		:	
		N0013 →	N0013_0001.png ... N0013_0006.png
	Settings →	S0001 →	S0001_0001.png ... S0001_0018.png
		:	
		S0007 →	S0007_0001.png ... S0007_0029.png

Fig. 2.3 Some X-ray images of an aluminum wheel (group Castings series C0001)

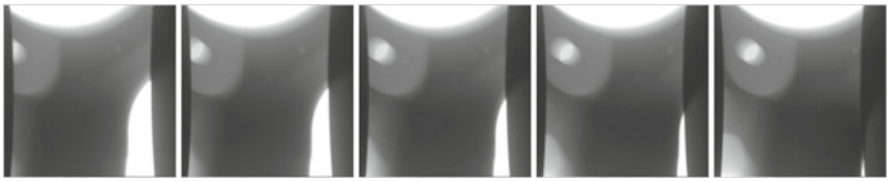

Fig. 2.4 Some X-ray images of a knuckle (group Castings series C0059)

given in Table A.2. Experiments on these data can be found in several publications as shown in Table 2.3. It is interesting to highlight that series C0001 (see Fig. 2.3) contains not only a sequence of 72 X-ray images taken from an aluminum wheel by rotating its central axis in 5°, but also annotations of bounding boxes of the ground truth of 226 small defects and the calibration matrix of each image that relates the 3D coordinates of the aluminum wheel with 2D coordinates of the X-ray image.

Table 2.3 Applications of series Castings

Series	Application	References
C0001	Detection of defects in multiple views	[2–7]
	Estimation of epipolar geometry with distortion	[8]
	Calibration of X-ray imaging system with image intensifiers	[2]
	Simulation of casting defects	[2]
C0002	Experiments on detection of defects in single views	[9–12]
C0008	Simulation of casting defects	[13]
C0017	Simulation of casting defects	[14, 15]
C0032	Experiments on detection of defects in multiple views	[3]
C0037	Simulation of casting defects	[14, 15]
C0049	Image restoration in blurred X-ray images	[16]
C0054	Detection of casting on moving castings	[17]
C0055	Image restoration in blurred X-ray images	[16]

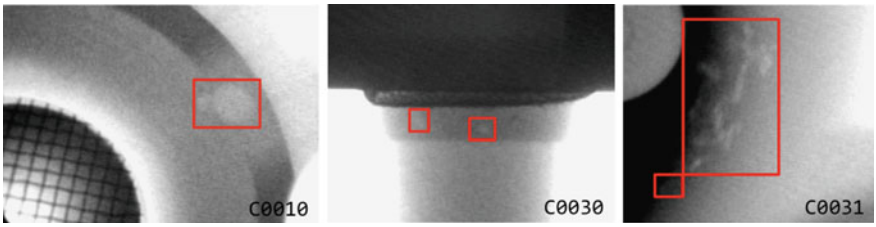

Fig. 2.5 Some annotated images showing bounding boxes of casting defects

2.4 Welds

The group Welds contains 88 images arranged in 3 series. The X-ray images were taken by the Federal Institute for Materials Research and Testing, Berlin (BAM).[5] Some examples are illustrated in Fig. 2.6. The details of each series are given in Table A.4. Experiments on these data can be found in several publications as shown in Table 2.4. It is interesting to highlight that series W0001 and W0002 (see Fig. 2.7) contains not only 10 X-ray images selected from the whole BAM database (series W0003), but also annotations of bounding boxes and the binary images of the ground truth of 641 defects.

[5]The X-ray images of series W0001 and W0003 are included in GDXray thanks to the collaboration of the Institute for Materials Research and Testing (BAM), Berlin http://dir.bam.de/dir.html.

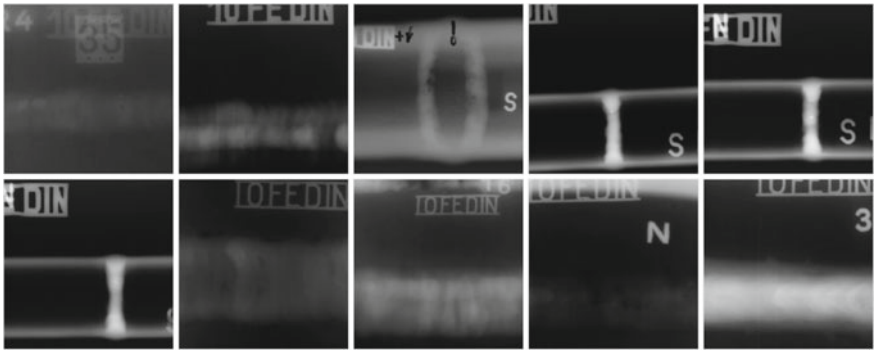

Fig. 2.6 Some X-ray images of group `Welds` series `W0003`. This series corresponds to the BAM database

Table 2.4 Applications of series Welds

Series	Application	References
`W0001`	Detection of defects in welds	[18–21]
	Simulation of welding defects	[15, 20]
`W0002`	Evaluation of performance of detection algorithm	[18]
`W0003`	Detection of defects in welds	[22, 23]

2.5 Baggage

The group Baggage contains 8,150 X-ray images arranged in 77 series. The X-ray images were taken from different containers such as backpacks, pen cases, wallets, etc. Some examples are illustrated in Figs. 2.8, 2.9 and 2.10. The details of each series are given in Table A.3. Experiments on these data can be found in several publications as shown in Table 2.5. It is interesting to highlight that series `B0046`, `B0047` and `B0048` (see for example Fig. 2.8) contains 600 X-ray images that can be used for automated detection of handguns, shuriken and razor blades (bounding boxes for these objects of interest are available as well). In this case, the training can be performed using series `B0049`, `B0050`, and `B0051` that includes X-ray images of individual handguns, shuriken and razor blades respectively taken from different points of view as shown in Fig. 2.9.

2.6 Natural Objects

The group Nature contains 8,290 X-ray images arranged in 13 series. The X-ray images were taken from different natural objects such as salmon filets, fruit, and wood pieces. Some examples are illustrated in Figs. 2.11, 2.12 and 2.13. The details

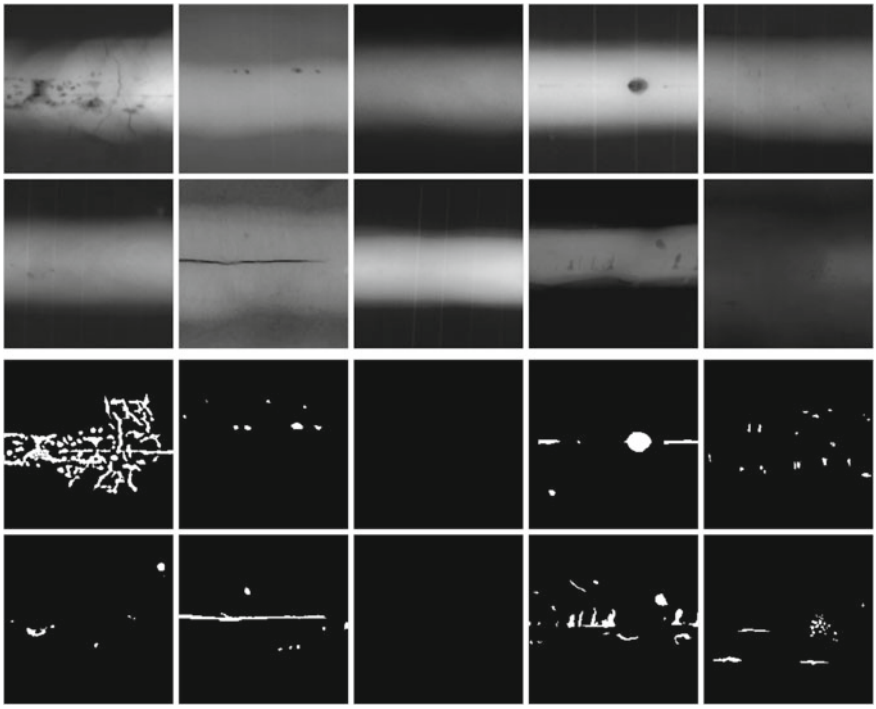

Fig. 2.7 Some images of group `Welds` series `W0001` (X-ray images) and `W0002` (ground truth)

Fig. 2.8 Some X-ray images of a bag containing handguns, *shuriken* and razor blades (group `Baggage` series `B0048`)

of each series are given in Table A.1. Experiments on these data can be found in several publications as shown in Table 2.6. It is interesting to highlight that series `N0012` and `N0013` (see Fig. 2.14) contains not only six X-ray images of salmon filets, but also annotations of bounding boxes and the binary images of the ground

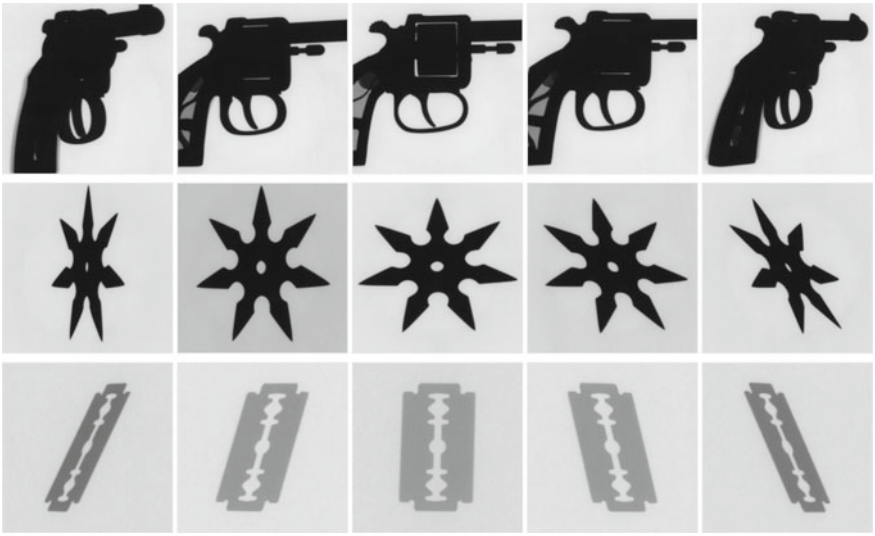

Fig. 2.9 Some X-ray images of handguns (series B0049), *shuriken* (series B0050) and razor baldes (series B0051) of group Baggage

Table 2.5 Applications of series Baggage

Series	Application	References
B0005	Experiments on detection of pins in multiple views	[3, 24]
	Detection of razor blades using active vision	[24]
B0007	Training of a classifier of razor blades	[24]
B0009-43	Experiments on detection of handguns	[25, 26]
B0045	Experiments on detection of objects in multiple views	[27, 28]
	Active vision	[24]
B0055	Experiments on detection of objects in sequences of four views	[27]
B0056	Experiments on detection of objects in sequences of six views	[27]
B0057	Experiments on detection of objects in sequences of eight views	[27]
B0058	Training of a classifier for clips, springs, and razor blades	[27, 28]
B0061-73	Detection of razor blades using active vision	[24]

truth of 73 fish bones. For training purposes, there are more than 7,500 labeled small crops (10 $\times$ 10 pixels), of regions of X-ray of salmon filets with and without fish bones in series N0003.

2.7 Settings

The group Settings contains 151 X-ray images arranged in 7 series. The X-ray images were taken from different calibration objects such checkerboards and 3D objects with regular patterns. Some examples are illustrated in Figs. 2.15 and 2.16. The details

Fig. 2.10 A knife was rotated in 1° and by each position an X-ray image was captured. In this figure, X-ray images at 0°, 10°, 20°, ... 350° are illustrated (see series `B00008` of group `Baggage`)

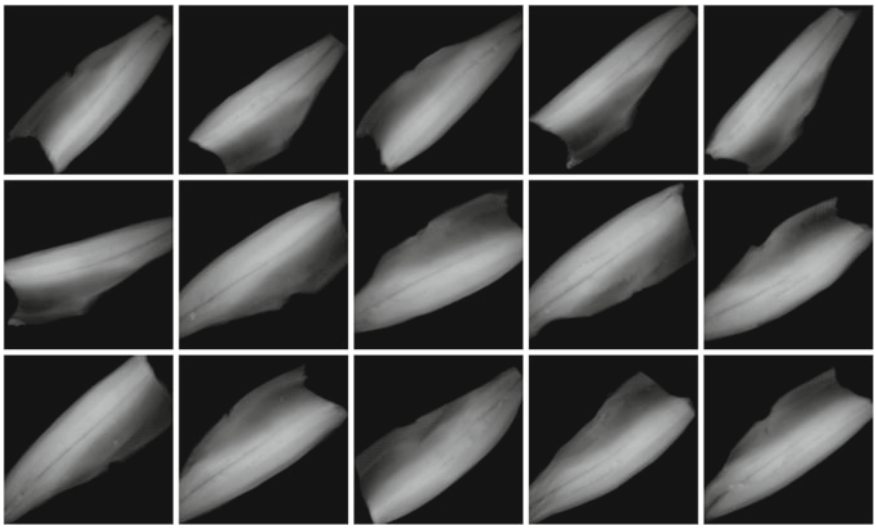

Fig. 2.11 Some X-ray images of salmon filets (group `Nature` series `N0011`)

of each series are given in Table A.5. Experiments on these data can be found in several publications as shown in Table 2.7. It is interesting to highlight that series `S0001` (see Fig. 2.15) contains not only 18 X-ray images of a copper checkerboard, but also the calibration matrix of each view. In addition, series `S0007` can be used for modeling the distortion of an image intensifier. The coordinates of each hole of the calibration pattern in each view are available, and the coordinates of the 3D model are given as well.

2.8 Matlab Commands

In order to manipulate $\mathbb{GDX}$ray database easily, some helpful Matlab commands were developed in $\mathbb{X}$VIS Toolbox. In this section, we present a summary of them with some examples.

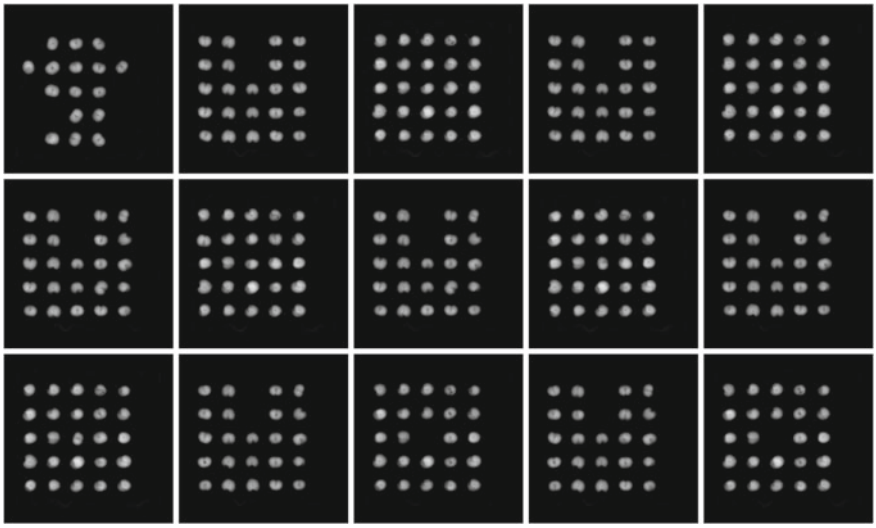

Fig. 2.12 Some X-ray images of cherries (group `Nature` series `N0006`)

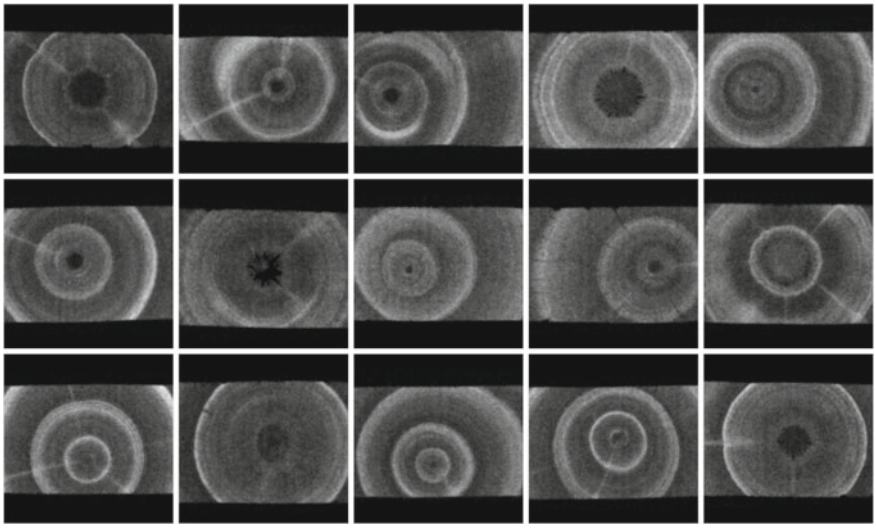

Fig. 2.13 Some X-ray images of wood (group `Nature` series `N0010`)

- Xgdxbrowse (see Appendix B): This GUI function[6] is used to browse $\mathbb{GDX}$ray database. An example is illustrated in Fig. 2.17. An additional example using pseudo-coloring is shown in Fig. 2.18, the user can select one of 10 different color maps.
- Xshowseries (see Appendix B): This function is used to display several images of a series in only one figure. For example, Fig. 2.10 was obtained using command:

[6] GUI: Graphic User Interface.

Table 2.6 Applications of series Nature

Series	Application	References
N0003	Automated design of a visual food quality system	[29]
N0003	Automated fish bone detection	[30]
N0008	Quality control of kiwis	[31]
N0011	Automated fish bone detection	[30]

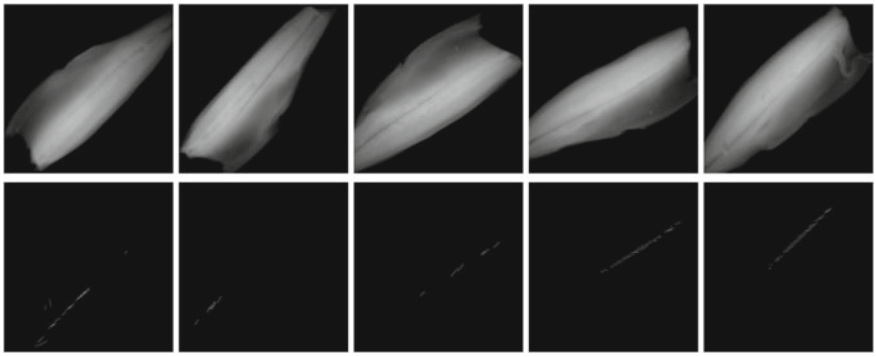

Fig. 2.14 Some images of group Nature series S0012 (X-ray images of salmon filets) and S0013 (ground truth for fish bones)

```
I = Xshowseries('B',8,1:10:351,18,0.2);
```

In this example, the images $1, 11, \ldots, 351$ of the eighth series of group 'B' are displayed using 18 images per row, and a new size per image scaled to 0.2 of the original size. The output is stored in matrix I.

- Xgdxdir (see Appendix B): This function is used to ascertain the path of a series of GDXray. For example, the directory of series N0012 can be obtained with command:

```
str = Xgdxdir('N',12);
```

- Xgdxstats (see Appendix B): This function is used to compute some statistics of GDXray. The output is Table 2.1.
- Xloadimg (see Appendix B): This function is used to load an image of GDXray. For example, N0012_0004.png can be stored in matrix I using command:

```
I = Xloadimg('N',12,4,1);
```

In this example, the last parameter can be '1' or '0', if the user wants to display the image or not.

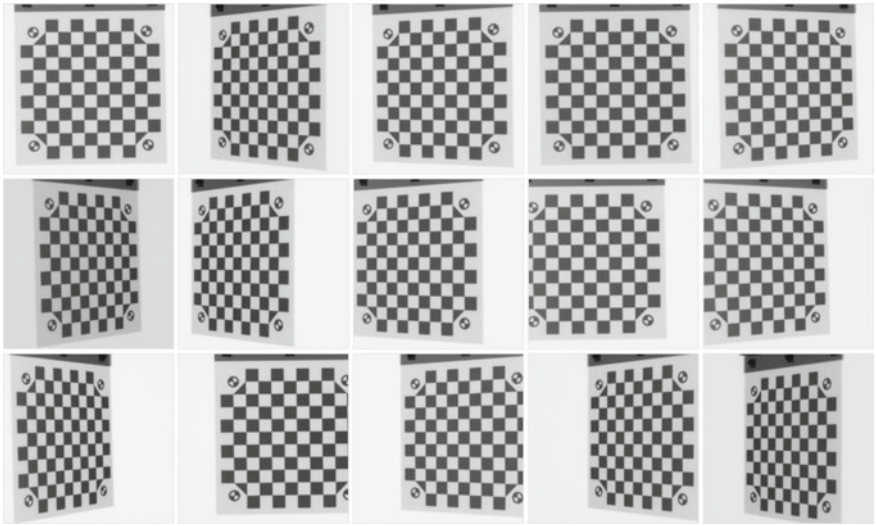

Fig. 2.15 Some X-ray images of a copper checkerboard used by calibration (group `Settings` series `S0001`)

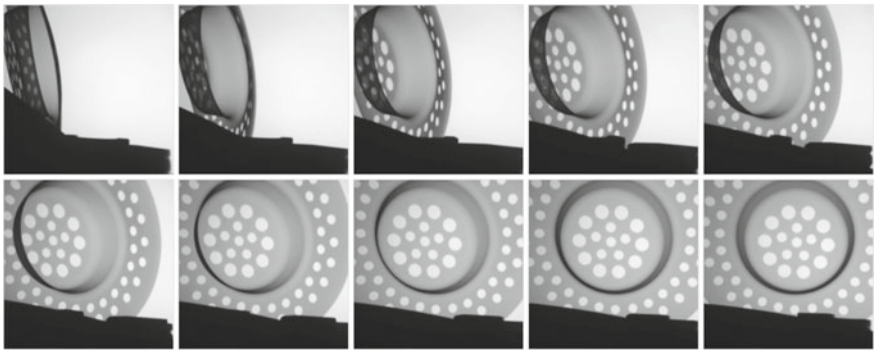

Fig. 2.16 Some X-ray images of circular pattern in different points of view used by calibration (group `Settings` series `S0007`)

Table 2.7 Applications of series Settings

Series	Application	References
`S0001`	Calibration of a multiple view X-ray imaging system for active vision	[24]
`S0002`	Distortion model of an image intensifier	[2, 8]
`S0007`	Explicit geometric model of a radioscopic imaging system	[32]

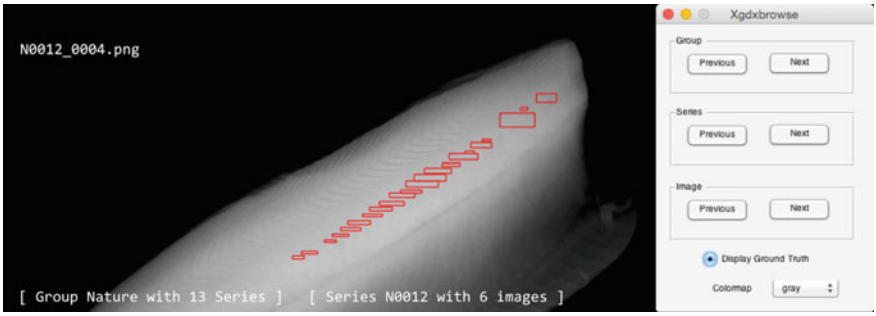

Fig. 2.17 Example of command Xgdxbrowse (see Appendix B) that can be used to browse GDXray. The user can click buttons `[Previous]` and `[Next]` to display the next groups, series or images. In addition, the ground truth option can be used to display manual annotations when they are available. In this example, the fish bones of a salmon filet are highlighted. For colored images see Fig. 2.18

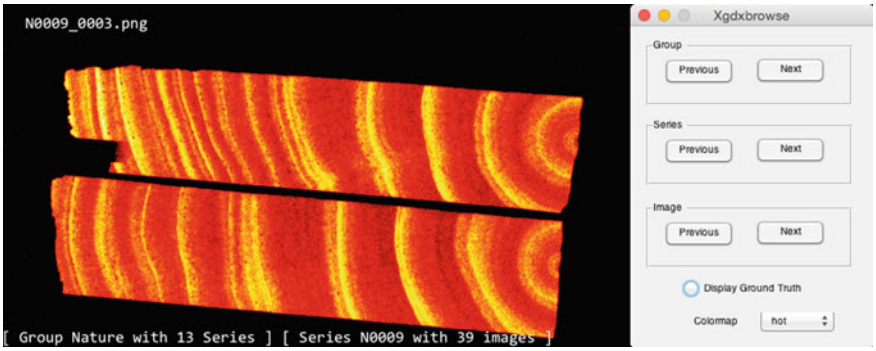

Fig. 2.18 Example of command Xgdxbrowse (see Appendix B) using pseudo coloring of a wood X-ray image. For another example in grayscale see Fig. 2.17

- XshowGT (see Appendix B): This function is used to display the bounding boxes of an X-ray image. For example, in figure `N0012_0004.png` the bounding boxes of the ground truth (see Fig. 2.17) can be displayed using command:

```
[I,bb] = XshowGT('N',12,4,'ground_truth.txt');
```

  In this example, image `N0012_0004.png` is stored in matrix `I`, and each bounding box in a row of matrix `bb`. The ground truth was previously stored in ASCII file `ground_truth.txt`. The format of this file is as follows: one bounding box per row; the first number of the row is the number of the image of the series, and the next four values are the coordinates x_1, x_2, y_1, y_2 of a bounding box. Thus, the rectangle of a bounding box is defined by its opposite vertices: (x_1, y_1) and (x_2, y_2). Another example is given in Fig. 2.5.

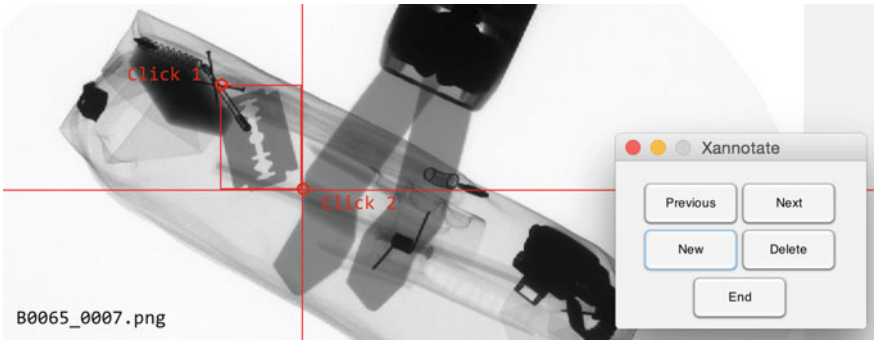

Fig. 2.19 Example of command Xgdxannotate (see Appendix B) that can be used to manually annotate the ground truth of a series. In this example, the user is annotating the razor blades of series `B0065`. With buttons `[Previous]` and `[Next]`, the user can browse the series. Button `[New]` is used to define a new bounding box in the current image by giving two clicks (the *red* axes can help to define the vertices of the bounding box). Button `[Delete]` is used to delete the last defined bounding box

- Xloaddata (see Appendix B): This function is used to load a file into workspace. For instance, the ground truth data of series `N0012` can be stored in matrix `GT` using command:

```
GT = Xloaddata('N',12,'ground_truth.txt');
```

- Xgdxannotate (see Appendix B): This function is used to manually annotate bounding boxes of a series of GDXray. Function Xgdxannotate (see Appendix B) calls GUI function Xannotate (see Appendix B) that is used to annotate the images of current directory. See an example in Fig. 2.19.

2.9 Summary

In this chapter, we presented the details of a new public dataset called GDXray. It consists of more than 19,400 X-ray images. The database includes five groups of X-ray images: castings, welds, baggage, natural objects, and settings. Each group has several series and X-ray images with many labels and annotations that can be used for training and testing purposes in computer vision algorithms. To the best knowledge of the author, up until now there have not been any public databases of digital X-ray images for X-ray testing.

In this chapter, we explained the structure of the GDXray database, we gave a description for each group (with some series examples), we presented some examples of applications that have been published using images of GDXray, and some examples in Matlab with XVIS Toolbox, that can be used to manipulate the database.

We believe that GDXray represents a relevant contribution to the X-ray testing community. On the one hand, students, researchers, and engineers can use these X-ray images to develop, test, and evaluate image analysis and computer vision algorithms without purchasing expensive X-ray equipment. On the other hand, these images can be used as a benchmark in order to test and compare the performance of different approaches on the same data. Moreover, the database can be used in the training programs of human inspectors.

References

1. Mery, D., Riffo, V., Zscherpel, U., Mondragon, G., Lillo, I., Zuccar, I., Lobel, H., Carrasco, M.: GDXray: The GRIMA database of X-ray images (http://dmery.ing.puc.cl/index.php/material/gdxray/) (2015)
2. Mery, D., Filbert, D.: Automated flaw detection in aluminum castings based on the tracking of potential defects in a radioscopic image sequence. IEEE Trans. Robot. Autom. **18**(6), 890–901 (2002)
3. Mery, D.: Automated detection in complex objects using a tracking algorithm in multiple X-ray views. In: Proceedings of the 8th IEEE Workshop on Object Tracking and Classification Beyond the Visible Spectrum (OTCBVS 2011), in conjunction with CVPR 2011, pp. 41–48. Colorado Springs (2011)
4. Carrasco, M., Mery, D.: Automatic multiple view inspection using geometrical tracking and feature analysis in aluminum wheels. Mach. Vis. Appl. **22**(1), 157–170 (2011)
5. Pizarro, L., Mery, D., Delpiano, R., Carrasco, M.: Robust automated multiple view inspection. Pattern Anal. Appl. **11**(1), 21–32 (2008)
6. Pieringer, C., Mery, D.: Flaw detection in aluminium die castings using simultaneous combination of multiple views. Insight **52**(10), 548–552 (2010)
7. Mery, D., Carrasco, M.: Automated multiple view inspection based on uncalibrated image sequences. Lect. Notes Comput. Sci. **3540**, 1238–1247 (2005)
8. Mery, D., Filbert, D.: The epipolar geometry in the radioscopy: Theory and application. at–Automatisierungstechnik **48**(12), 588–596 (2000). (in German)
9. Mery, D.: Crossing line profile: a new approach to detecting defects in aluminium castings. In: Proceedings of the Scandinavian Conference on Image Analysis (SCIA 2003), Lecture Notes in Computer Science **2749**, 725–732 (2003)
10. Ghoreyshi, A., Vidal, R., Mery, D.: Segmentation of circular casting defects using a robust algorithm. Insight-Non-Destruct. Test. Cond. Monit. **47**(10), 615–617 (2005)
11. Ramírez, F., Allende, H.: Detection of flaws in aluminium castings: a comparative study between generative and discriminant approaches. Insight-Non-Destruct. Test. Cond. Monit. **55**(7), 366–371 (2013)
12. Mery, D., Chacón, M., Munoz, L., González, L.: Automated inspection of aluminium castings using fusion strategies. Mater. Eval. (2005). In Press
13. Huang, Q., Wu, Y., Baruch, J., Jiang, P., Peng, Y.: A template model for defect simulation for evaluating nondestructive testing in X-radiography. IEEE Trans. Syst., Man Cybern., Part A: Syst. Hum. **39**(2), 466–475 (2009)
14. Mery, D.: A new algorithm for flaw simulation in castings by superimposing projections of 3D models onto X-ray images. In: Proceedings of the XXI International Conference of the Chilean Computer Science Society (SCCC-2001), pp. 193–202. IEEE Computer Society Press, Punta Arenas (2001)
15. Mery, D., Hahn, D., Hitschfeld, N.: Simulation of defects in aluminum castings using CAD models of flaws and real X-ray images. Insight **47**(10), 618–624 (2005)

16. Mery, D., Filbert, D.: A fast non-iterative algorithm for the removal of blur caused by uniform linear motion in X-ray images. In: Proceedings of the 15th World Conference on Non-Destructive Testing (WCNDT-2000). Rome (2000)
17. Mery, D., Filbert, D.: Automated inspection of moving aluminium castings. In: 8th European Conference on Non-Destructive Testing (ECNDT 2002). Barcelona (2002)
18. Carrasco, M., Mery, D.: Segmentation of welding defects using a robust algorithm. Mater. Eval. **62**(11), 1142–1147 (2004)
19. Mery, D., Berti, M.A.: Automatic detection of welding defects using texture features. Insight-Non-Destruct. Test. Cond. Monit. **45**(10), 676–681 (2003)
20. Mery, D.: Automated detection of welding defects without segmentation. Mater. Eval. **69**(6), 657–663 (2011)
21. Hernández, S., Sáez, D., Mery, D., da Silva, R., Sequeira, M.: Automated defect detection in aluminium castings and welds using neuro-fuzzy classifiers. In: Proceedings of the 16th World Conference on Non-Destructive Testing (WCNDT-2004). Montreal (2004)
22. Perner, P., Zscherpel, U., Jacobsen, C.: A comparison between neural networks and decision trees based on data from industrial radiographic testing. Pattern Recognit. Lett. **22**(1), 47–54 (2001)
23. da Silva, R.R., Siqueira, M.H., de Souza, M.P.V., Rebello, J.M., Calôba, L.P.: Estimated accuracy of classification of defects detected in welded joints by radiographic tests. NDT & E Int. **38**(5), 335–343 (2005)
24. Riffo, V., Mery, D.: Active X-ray testing of complex objects. Insight **54**(1), 28–35 (2012)
25. Mery, D., Riffo, V., Mondragon, G., Zuccar, I.: Detection of regular objects in baggages using multiple X-ray views. Insight **55**(1), 16–21 (2013)
26. Damashek, A., Doherty, J.: Detecting guns using parametric edge matching. Technical Report Project for Computer Vision Course: CS231A, Stanford University (2015)
27. Mery, D.: Inspection of complex objects using multiple-X-ray views. IEEE/ASME Trans. Mechatron. **20**(1), 338–347 (2015)
28. Mery, D., Riffo, V., Zuccar, I., Pieringer, C.: Automated X-ray object recognition using an efficient search algorithm in multiple views. In: Proceedings of the 9th IEEE CVPR Workshop on Perception Beyond the Visible Spectrum, Portland (2013)
29. Mery, D., Pedreschi, F., Soto, A.: Automated design of a computer vision system for visual food quality evaluation. Food Bioprocess Techol. **6**(8), 2093–2108 (2013)
30. Mery, D., Lillo, I., Riffo, V., Soto, A., Cipriano, A., Aguilera, J.: Automated fish bone detection using X-ray testing. J. Food Eng. **2011**(105), 485–492 (2011)
31. Mondragón, G., Leiva, G., Aguilera, J., Mery, D.: Automated detection of softening and hard columella in kiwifruits during postharvest using X-ray testing. In: Proceedings of International Congress on Engineering and Food (2011)
32. Mery, D.: Explicit geometric model of a radioscopic imaging system. NDT & E Int. **36**(8), 587–599 (2003)

http://www.springer.com/978-3-319-20746-9

Computer Vision for X-Ray Testing
Imaging, Systems, Image Databases, and Algorithms
Mery, D.
2015, XXIV, 347 p. 311 illus., 62 illus. in color.,
Hardcover
ISBN: 978-3-319-20746-9